RAA 2020 Vol. **20** No. **11**, 175(9pp) doi: 10.1088/1674-4527/20/11/175

http://www.raa-journal.org *http://iopscience.iop.org/raa*

Research in Astronomy and Astrophysics

Accretion flow properties of XTE J1118+480 during its 2005 outburst

Dipak Debnath[1], Debjit Chatterjee[1], Arghajit Jana[1,2], Sandip K. Chakrabarti[1] and Kaushik Chatterjee[1]

[1] Indian Centre for Space Physics, 43 Chalantika, Garia St. Rd., Kolkata, 700084, India; *dipakcsp@gmail.com*
[2] Physical Research Laboratory, Navrangpura, Ahmedabad 380009, India

Received 2020 January 3; accepted 2020 April 5

Abstract We study spectral and temporal properties of Galactic short orbital period transient black hole XTE J1118+480 during its 2005 outburst using archival data of RXTE PCA and HEXTE instruments in the combined energy range of $3 - 100$ keV. Spectral analysis with the physical two component advective flow (TCAF) model allows us to understand the accretion flow properties of the source. We found that this outburst of XTE J1118+480 is an unconventional outburst as the source was only in the hard state (HS). Our spectral analysis suggests that during the entire outburst, the source was highly dominated by the low angular momentum sub-Keplerian halo rate. Since the source was active in radio throughout the outburst, we make an effort to estimate X-ray contribution of jets to total observed X-ray emissions from the spectral analysis with the TCAF model. The total X-ray intensity shows a similar nature of evolution as that of radio and jet X-ray fluxes. This allowed us to define this 'outburst' also as a jet dominated 'outburst'. Total X-ray flux is also found to subside when jet activity disappears. Our detailed spectral analysis also indicated that although the source was only in the HS during the outburst, in the late declining phase the spectrum became slightly softer due to the slow rise in the Keplerian disk rate.

Key words: X-Rays: binaries — stars: black holes — stars individual: (XTE J1118+480) — accretion, accretion disks — ISM: jets and outflows — radiation: dynamics

1 INTRODUCTION

XTE J1118+480 was discovered on 2000 March 29 by the *All Sky Monitor* (ASM) onboard the Rossi X-ray Timing Explorer (RXTE) satellite at R.A.= $11^{\rm h}18^{\rm m}10^{\rm s}.79$, Dec.= $48°02'12''.42$ (Remillard et al. 2000). Follow up observations were carried out by Uemura et al. 2000; Chaty et al. 2000; Wren & McKay 2000; Mauche et al. 2000; Pooley & Waldram 2000. Because of its unique position in the Galactic halo, this black hole (BH) binary suffered much less absorption and is widely studied in multi-wavelengths during both its active outbursting periods and in its quiescent state (Revnivtsev et al. 2000; Cook et al. 2000; Garcia et al. 2000; Haswell et al. 2000; Hynes et al. 2000; McClintock et al. 2000; Wagner et al. 2000; Taranova & Shenavrin 2000; Esin et al. 2001; Markoff et al. 2001; Hynes et al. 2003; Chaty et al. 2003; Shahbaz et al. 2005). The distance of this system is estimated to be around 1.8 kpc (McClintock et al. 2001a). The distance above the Galactic plane ($\sim$ 1.7 kpc) places it in the 'Lockman halo' (Uemura et al. 2000). Quasi-Periodic Oscillations (QPOs) were observed in X-ray, optical and extreme ultraviolet (EUV) (Wood et al. 2000; Haswell et al. 2000). The mass of the BH has been predicted dynamically by Wagner et al. (2001) ($6.0 - 7.7\,M_{\odot}$), Gelino et al. (2006) ($8.53 \pm 0.6\,M_{\odot}$) and Khargharia et al. (2013) ($6.9 - 8.2\,M_{\odot}$). This is suggested to be a highly inclined ($\sim 68° - 79°$) (Khargharia et al. 2013), short orbital period ($\sim$ 4.1 h) (Patterson et al. 2000; González Hernández et al. 2012) low mass binary system. The spectral and temporal properties of the source during its 2000 outburst have been studied by Chatterjee et al. (2019) (hereafter Paper-I), utilizing combined RXTE Proportional Counter Array (PCA) and High Energy X-ray Timing Experiment (HEXTE) data with the physical two component advective flow (TCAF) model (Chakrabarti & Titarchuk 1995) to understand the accretion flow dynamics of the source. Estimation of the X-ray contribution of the jet made from spectral analysis with the TCAF model suggests that the outburst was dominated by jets/outflows. Monotonic evolution of low frequency QPOs is also studied. In Paper-I, the probable mass of the BH is also estimated from the spectral analysis in the range of $6.25 - 7.49\,M_{\odot}$ or $6.99^{+0.50}_{-0.74}\,M_{\odot}$.

After roughly five years in the quiescent phase in January 2005, XTE J1118+480 exhibited new outbursting activity with shorter duration ($\sim$ 1.5 months) and lower intensity flux compared to its earlier (2000) outburst. Multi-wavelength studies of the source during this outburst are also carried out by many authors. Zurita et al. (2005b) reported an optical outburst on 2005 January 9. The outburst was also detected at X-ray and radio wavelengths (Remillard et al. 2005; Pooley 2005; Rupen et al. 2005). The outburst faded rapidly and reached near quiescence by late February (Zurita et al. 2005a). The evolution of the long-term lightcurve and outburst properties was discussed by Zurita et al. (2006).

In the present paper, our goal is to study accretion flow properties of the source during its 2005 outburst. We wanted to check whether the nature of the source is similar to other shorter orbital period harder or type-II transient low-mass X-ray binaries recently studied by our group (see Debnath et al. 2017 and references therein). Here, we also make an effort to study properties of jets, particularly in the X-ray band. A detailed spectral analysis is made applying the physical TCAF model (Chakrabarti & Titarchuk 1995), which is based on transonic flows (Chakrabarti 1997). This TCAF configuration consists of two types of flows, namely, high viscous, high angular momentum Keplerian flow along the equatorial plane and low viscous, low angular momentum sub-Keplerian flow enveloping the Keplerian disk. Close to the BH, an axisymmetric shock forms due to the centrifugal barrier and the supersonic sub-Keplerian flow suddenly jumps to the subsonic branch. The post-shock region puffs-up and becomes hot due to slowing down of the matter at the shock location. This puffed-up region between the shock and the inner sonic point just outside of the horizon acts as the Compton cloud. This is known as the CENtrifugal pressure supported BOundary Layer or CENBOL. Thermal soft photons from the Keplerian disk become hard via repeated inverse-Compton scattering in the region. Although this generalized accretion flow model was introduced more than two decades ago, its recent implementation (after generation of model *fits* file using $\sim 10^6$ theoretical spectra produced by varying five model input parameters) as an additive table into HEASARC's spectral analysis software package XSPEC allowed one to gain a clearer picture about the flow dynamics of several BH sources (Debnath et al. 2014, 2015b,a, 2017; Mondal et al. 2014, 2016; Jana et al. 2016; Jana et al. 2020a; Chatterjee et al. 2016, 2019; Molla et al. 2017). Masses of a few black hole candidates (BHCs) have been measured to a better accuracy from normalization independent spectral analysis with the TCAF model (Molla et al. 2016, 2017; Chatterjee et al. 2016, 2019, 2020; Jana et al. 2016; Jana et al. 2020a; Debnath et al. 2017; Bhattacharjee et al. 2017; Shang et al. 2019). Theoretically, the coupling of disk and jet connection has been studied based on the transonic flow model by several authors (Chakrabarti 1999a,b; Chattopadhyay & Das 2007; Aktar et al. 2015). The outflow rate from the inflowing accretion rate has been calculated implementing hydrodynamics of infalling and outgoing transonic flows (Chakrabarti 1999a,b; Das & Chakrabarti 1999). Chakrabarti & Mandal (2006) studied the two component accretion flows in the presence of synchrotron radiation. Estimation of the contribution of the jet X-ray fluxes (if present) and their properties is also studied with the TCAF model (Jana et al. 2017, 2020b; Paper-I). Even frequencies of the dominating type-C QPOs are also predicted from the TCAF model fitted shock parameters (Debnath et al. 2014; Chatterjee et al. 2016).

This paper is organized in the following way: in Section 2, we discuss the observation and data analysis procedures. In Section 3, we present the results from our spectral analysis using two types of models. Evolution of X-ray contribution of jets/outflows during the outburst is studied with that of radio fluxes. Finally, in Section 4, we summarize the result and briefly present a comparison between this and the 2000 outburst.

2 OBSERVATIONS AND DATA ANALYSIS

In 2005, although the outburst was reported on January 9 by Zurita et al. (2005b), RXTE started monitoring it five days later on a daily basis. To find the broad spectral information in the $3 - 100$ keV band, we studied 21 observations of combined data of RXTE PCA and HEXTE instruments from 2005 January 14 (MJD=53384.99) to January 25 (MJD=53395.59). HEASARC's software package HeaSoft version HEADAS 6.16 and XSPEC version 12.8 was employed for our analysis. We followed the methods mentioned in Debnath et al. (2013, 2015b) for data reduction and analysis.

The RXTE PCA lightcurves in the energy range of $2 - 15$ keV and $2 - 25$ keV are generated considering the event mode data with a maximum time resolution of 125 μs. The power density spectra (PDSs) are generated using XRONOS task 'powspec' on 0.01 s binned lightcurves. We utilized 1 sec time binned background subtracted lightcurves of the Proportional Counter Unit 2 (PCU2) to calculate average PCA count rate in 2–25 keV for each observation.

In general, PCU2 data of 'standard 2' mode (FS4a* in the energy range $3 - 25$ keV) and HEXTE science mode data (FS52* in the energy range of $20 - 100$ keV) of Cluster 0 or A are utilized for spectral analysis. For

some observations due to low signal to noise ratio (S/N), we consider HEXTE data only in the $20 - 40$ keV band. The background subtracted spectra were first fitted with a single power law (PL) model, verifying that no significant thermal disk blackbody (DBB) component was required. After that, we refitted all the spectra using the TCAF solution based on an additive table *fits* file. A fixed hydrogen column density $N_H = 1.3 \times 10^{20}\,\mathrm{atoms\,cm^{-2}}$ is input for photoelectric absorption model *phabs* (Garcia et al. 2000; McClintock et al. 2001b). A 0.5% systematic error is considered during spectral analysis with the PL as well as the TCAF model.

To fit a spectrum with the TCAF model, four flow parameters are required. These parameters are: two types of accretion rates: (i) Keplerian disk rate ($\dot{m}_d$ in Eddington rate $\dot{M}_{\rm Edd}$), (ii) sub-Keplerian halo rate ($\dot{m}_h$ in $\dot{M}_{\rm Edd}$) and two shock parameters: (iii) shock location (X_s in Schwarzschild radius $r_s = 2GM_{\rm BH}/c^2$) and (iv) compression ratio ($R = \rho_+/\rho_-$, where ρ_+ and ρ_- are the densities of post- and pre- shock regions respectively). In addition, if the mass of the BH ($M_{\rm BH}$ in $M_\odot$) is known, one needs to provide the value of the mass and keep it frozen. Otherwise, each fitted spectrum returns a value of the mass. One also gets a normalization (N) from each fitting. This normalization parameter is a function of the mass of the BH ($M_{\rm BH}$), the distance (D) of the system and the inclination angle (i) of the disk. So for a specific BH, this normalization value is expected to be a constant parameter, if measured with a given instrument (Molla et al. 2016, 2017), excluding the facts that the system is not precessing and there is no significant jet/outflow from the disk. Jana et al. (2017) (hereafter JCD17) developed a method to estimate X-ray contribution of jets/outflows from spectral analysis with the TCAF model. They compared the variation of the model normalization with the observed radio fluxes, since radio emission is known to be a tracer of jets/outflows. If there is a significant X-ray contribution from jets, we may require a higher value of the normalization to fit a spectrum to take care of extra photon contributions from the base of the jets. While comparing N with the radio flux ($F_{\rm R}$), if lower N is found when $F_{\rm R}$ is also at its minimum, then it implies that during this low normalization time there is insignificant or no X-ray contribution from the jets in the net emission spectrum. In other words, a large amount of outflow results in higher values of N. They also prescribed the procedure to calculate the amount of X-ray outflow flux ($F_{\rm ouf}$). Following their method in Paper-I, Chatterjee et al. (2019) calculated jet X-ray fluxes during the 2000 outburst of XTE J1118+480, where the minimum value of N is observed at 4.36. Since the current outburst of XTE J1118+480 is also highly jet dominated, following the same method, we estimated the contribution of the jet X-ray flux to total flux for all observations.

Note: Since the main goal of this paper is not to measure the mass of the BH, we kept mass of the BH frozen at 7 $M_\odot$ while fitting energy spectra with the TCAF model. This is the mean value of the TCAF model fitted mass values obtained from the spectral analysis of the 2000 outburst of XTE J1118+480 (see Paper-I).

3 RESULTS

We study accretion properties of XTE J1118+480 during its 2005 outburst by analyzing 21 RXTE PCA and HEXTE observations, selected from 2005 January 14 (MJD=53384.99) to January 25 (MJD=53395.59). Both temporal and spectral properties of the source are investigated. Spectral study is done with the phenomenological (PL) and physical (TCAF) accretion flow models.

In Figure 1, one example of a PDS is depicted along with the TCAF fitted combined PCA plus HEXTE spectrum of the data with observation ID 90011–01–01–04. In Figure 2, variation of PCU2 count rate (in $2 - 25$ keV) and spectral parameters fitted with two different types of models: PL (PL flux, PL photon index Γ) and TCAF (Keplerian disk rate $\dot{m}_d$, sub-Keplerian halo rate $\dot{m}_h$, shock location X_s and compression ratio R) are featured. Since we have been able to separate total observed X-ray into its two constituents: contribution from $i)$ inflowing matter or accretion disk, and $ii)$ outflowing matter or jets; in Figure 3(a)-(c) we show variation of total X-ray flux (F_X), X-ray fluxes from accretion disk ($F_{\rm inf}$) and jets ($F_{\rm ouf}$). The variation of model normalization (N) and observed radio flux ($F_{\rm R}$) is also plotted in Figure 3(d)-(e). The radio flux ($F_{\rm R}$ in mJy) data of the 15 GHz Ryle Telescope are displayed here and are adopted from Brocksopp et al. (2010).

The detailed spectral analysis results are presented in Tables 1 and 2. In Table 1, both PL and TCAF model fitted spectral parameters are presented. Different types of X-ray fluxes (F_X, $F_{\rm inf}$, $F_{\rm ouf}$), the percentage of the contribution of the jet X-ray to total X-ray and TCAF model fitted normalization parameter values are presented in Table 2.

3.1 Temporal Study

RXTE PCA started to monitor the source five days later than the report of the outburst on 2005 January 9 by Zurita et al. (2005b). Since this is a Fast Rise Slow Decay (FRSD) type outburst (see Debnath et al. 2010), during the first PCA observation, the source already crossed its peak flux (see Fig. 2(a)). It manifested a monotonic decrease in

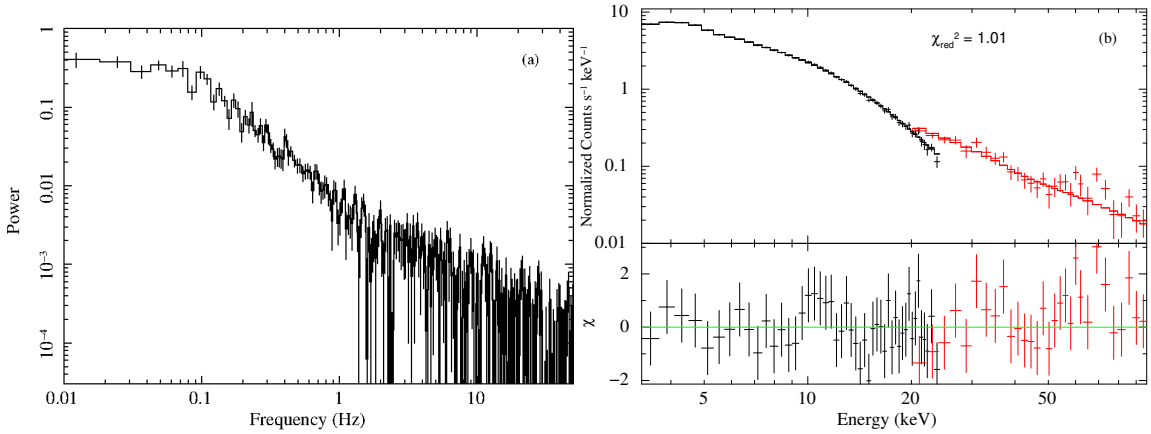

Fig. 1 (a) A sample PDS of 0.01 s time binned PCU2 lightcurve and (b) TCAF model fitted combined PCA plus HEXTE spectrum in the $3-100$ keV energy range for observation ID 90011-01-01-04 (MJD=53387.80) are displayed.

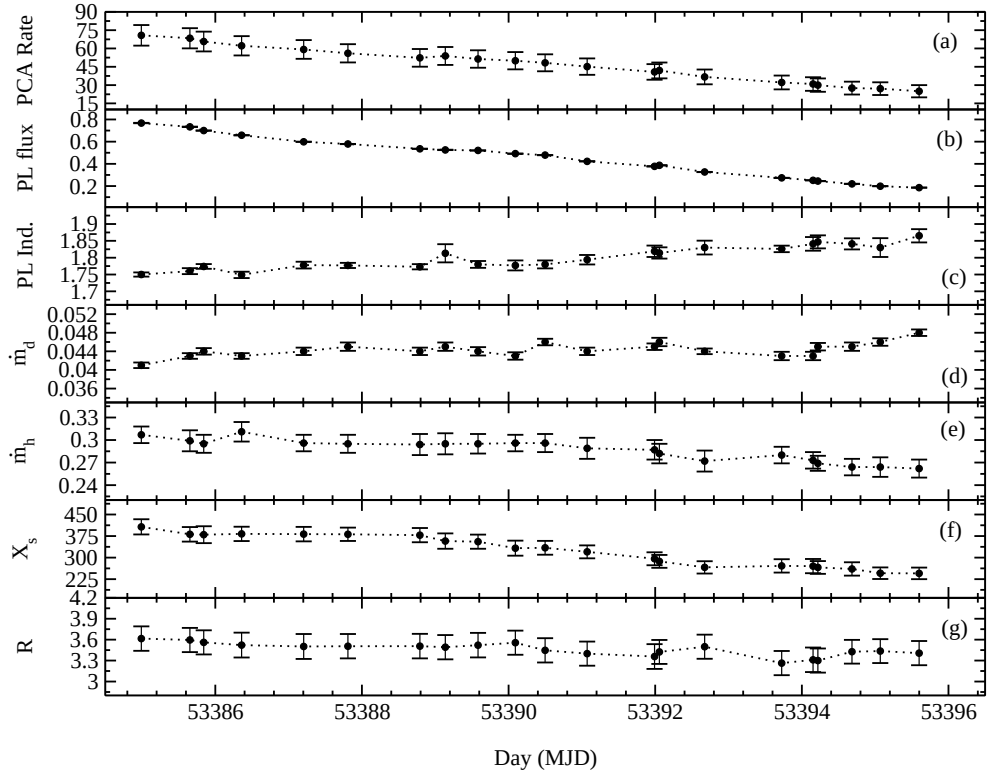

Fig. 2 Variation of (a) PCU2 count rate (count s^{-1}) in the $2-25$ keV energy range, PL model fitted (b) PL flux in units of 10^{-9} erg cm^{-2} s^{-1}, (c) PL photon index (Γ), TCAF model fitted (d) disk rate ($\dot{m}_d$) in $\dot{M}_{\rm Edd}$, (e) halo rate ($\dot{m}_h$) in $\dot{M}_{\rm Edd}$, (f) shock location (X_s) in r_s and (g) compression ratio (R) with day (in MJD) are plotted.

the PCU2 photon count rate in the $2-25$ keV energy band. Fourier transformed PDSs (see Fig. 1(a)) are generated for all observations using 0.01 s time binned $2-15$ keV lightcurves. We have not seen any prominent signature of the low frequency QPOs, which are generally observable during the outburst of this type of transient BHC. Contrary to this, monotonic evolution (increasing frequency from 0.06 to 0.16 Hz) of the QPOs was observed during the 2000 outburst of the source (see Paper-I). However, there is a report on the presence of a mHz QPO by Shahbaz et al. (2005) in the optical waveband on June 2003, which is the quiescent phase between 2000 and 2005 outbursts.

3.2 Spectral Study

The spectral analysis is done independently with the two types of models: i) phenomenological PL model and ii) physical TCAF model. While PL model fit gives us

Table 1 PL or TCAF Model Fitted Spectral Parameters

Obs. ID	UT Date	MJD	PL Ind (Γ)	PL flux	χ^2/dof	$\dot{m}_d$ ($\dot{M}_{\rm Edd}$)	$\dot{m}_h$ ($\dot{M}_{\rm Edd}$)	X_s (r_s)	R	χ^2/dof
(1)	(2)	(3)	(4)	(5)	(6)	(7)	(8)	(9)	(10)	(11)
X-01-00	14/01	53384.99	$1.750^{\pm0.006}$	$0.768^{\pm0.002}$	45.5/47	$0.041^{\pm0.0006}$	$0.30^{\pm0.011}$	$406^{\pm26}$	$3.61^{\pm0.17}$	89.4/68
X-01-07	15/01	53385.65	$1.760^{\pm0.008}$	$0.734^{\pm0.002}$	39.2/47	$0.043^{\pm0.0006}$	$0.29^{\pm0.014}$	$381^{\pm25}$	$3.59^{\pm0.17}$	65.2/68
X-01-02	15/01	53385.84	$1.774^{\pm0.007}$	$0.700^{\pm0.001}$	46.6/47	$0.044^{\pm0.0007}$	$0.29^{\pm0.012}$	$379^{\pm29}$	$3.56^{\pm0.17}$	68.0/71
X-01-08	16/01	53386.35	$1.749^{\pm0.009}$	$0.658^{\pm0.002}$	44.1/47	$0.043^{\pm0.0006}$	$0.31^{\pm0.013}$	$382^{\pm24}$	$3.52^{\pm0.17}$	69.5/71
X-01-09	17/01	53387.20	$1.778^{\pm0.010}$	$0.599^{\pm0.001}$	41.3/47	$0.044^{\pm0.0008}$	$0.29^{\pm0.011}$	$381^{\pm25}$	$3.50^{\pm0.17}$	62.4/71
X-01-04	17/01	53387.80	$1.777^{\pm0.007}$	$0.579^{\pm0.001}$	43.4/47	$0.045^{\pm0.0009}$	$0.29^{\pm0.012}$	$381^{\pm23}$	$3.50^{\pm0.17}$	68.7/68
X-01-05	18/01	53388.79	$1.773^{\pm0.007}$	$0.536^{\pm0.001}$	69.7/47	$0.044^{\pm0.0008}$	$0.29^{\pm0.014}$	$378^{\pm24}$	$3.50^{\pm0.17}$	97.4/71
X-01-11	19/01	53389.13	$1.813^{\pm0.027}$	$0.526^{\pm0.002}$	49.2/47	$0.045^{\pm0.0009}$	$0.29^{\pm0.014}$	$357^{\pm26}$	$3.49^{\pm0.17}$	44.9/40
X-01-12	19/01	53389.58	$1.780^{\pm0.010}$	$0.521^{\pm0.001}$	36.7/47	$0.044^{\pm0.0009}$	$0.29^{\pm0.013}$	$355^{\pm24}$	$3.52^{\pm0.17}$	42.1/51
X-01-13	20/01	53390.09	$1.777^{\pm0.014}$	$0.492^{\pm0.002}$	54.2/47	$0.043^{\pm0.0008}$	$0.29^{\pm0.011}$	$332^{\pm26}$	$3.55^{\pm0.17}$	62.4/51
X-01-06	20/01	53390.49	$1.780^{\pm0.011}$	$0.479^{\pm0.001}$	39.0/47	$0.046^{\pm0.0007}$	$0.29^{\pm0.012}$	$334^{\pm24}$	$3.44^{\pm0.17}$	46.7/46
Y-02-00	21/01	53391.07	$1.794^{\pm0.014}$	$0.423^{\pm0.002}$	43.9/47	$0.044^{\pm0.0008}$	$0.28^{\pm0.014}$	$319^{\pm22}$	$3.40^{\pm0.17}$	43.7/48
Y-02-02	21/01	53391.99	$1.819^{\pm0.017}$	$0.378^{\pm0.002}$	34.9/47	$0.045^{\pm0.0007}$	$0.28^{\pm0.013}$	$295^{\pm22}$	$3.35^{\pm0.17}$	36.6/46
Y-02-03	22/01	53392.05	$1.814^{\pm0.016}$	$0.387^{\pm0.002}$	25.4/47	$0.046^{\pm0.0009}$	$0.28^{\pm0.013}$	$286^{\pm22}$	$3.42^{\pm0.17}$	27.9/46
Y-02-04	22/01	53392.67	$1.830^{\pm0.020}$	$0.327^{\pm0.001}$	48.9/47	$0.044^{\pm0.0006}$	$0.27^{\pm0.014}$	$265^{\pm21}$	$3.49^{\pm0.17}$	56.2/46
Y-02-06	23/01	53393.72	$1.826^{\pm0.009}$	$0.274^{\pm0.001}$	51.3/47	$0.043^{\pm0.0009}$	$0.28^{\pm0.011}$	$271^{\pm23}$	$3.26^{\pm0.17}$	121/71
Y-02-14	24/01	53394.15	$1.841^{\pm0.020}$	$0.252^{\pm0.001}$	29.6/47	$0.043^{\pm0.0009}$	$0.27^{\pm0.011}$	$270^{\pm24}$	$3.31^{\pm0.17}$	34.2/46
Y-02-15	24/01	53394.21	$1.847^{\pm0.019}$	$0.245^{\pm0.001}$	38.5/47	$0.045^{\pm0.0008}$	$0.26^{\pm0.010}$	$265^{\pm22}$	$3.30^{\pm0.17}$	44.0/46
Y-02-07	24/01	53394.68	$1.841^{\pm0.016}$	$0.220^{\pm0.001}$	44.0/47	$0.045^{\pm0.0009}$	$0.26^{\pm0.011}$	$260^{\pm23}$	$3.42^{\pm0.17}$	33.6/46
Y-02-09	25/01	53395.06	$1.830^{\pm0.027}$	$0.199^{\pm0.001}$	42.5/47	$0.046^{\pm0.0008}$	$0.26^{\pm0.013}$	$245^{\pm20}$	$3.43^{\pm0.17}$	47.9/46
Y-02-10	25/01	53395.59	$1.865^{\pm0.019}$	$0.186^{\pm0.001}$	26.9/47	$0.048^{\pm0.0007}$	$0.26^{\pm0.012}$	$245^{\pm20}$	$3.40^{\pm0.17}$	26.1/43

X=90011-01, Y=90111-01 are prefixes of observation IDs. UT date is in dd/mm format of year 2005.
Γ represents the photon indices obtained from pure PL model fitting. PL flux indicates the flux from PL model in $10^{-9}\,{\rm erg\,cm^{-2}\,s^{-1}}$.
$\dot{m}_d$, $\dot{m}_h$, X_s and R are the TCAF fitted parameters. The accretion rates ($\dot{m}_d$ and $\dot{m}_h$) are in Eddington rate.
X_s is the shock location values in units of r_s and R is the compression ratio. PL and TCAF model fitted $\chi^2_{\rm red}$ values are mentioned as χ^2/dof in Cols. (6) and (11) respectively, where 'dof' represents the degrees of freedom. The superscripts are average error values of the $\pm$ 90% confidence errors, extracted using the 'err' task in XSPEC.

an overview about the spectral properties of the source during different phases of the outburst, TCAF model fitted physical flow parameters allow us to get the accretion flow dynamics and evolution of the flow geometry.

First, we fitted the background subtracted spectra solely with the PL model. No significant DBB contribution was noticed during the spectral fittings. Although low values of the PL photon indices ($\Gamma \sim 1.75 - 1.87$) are observed during the outburst, in the late declining phase, a slow increase in Γ values (from 1.81 to 1.87) is observed (see Fig. 2(c)). On the first observation (MJD= 53384.99) day, $\Gamma = 1.75$ is observed, and it varied in a narrow range of $\sim 1.75 - 1.81$ for the next seven days till MJD=53392.05 before rising slowly in the next three days to reach its maximum value of 1.87 on the last day (MJD=53395.59) of our observation. The observation of the low Γ signifies a hard spectral state, which is similar to what was seen during its earlier (2000) outburst of this source (Chaty et al. 2003; Paper-I). PL flux exhibited a similar nature of monotonic decrease in PCA count rate during the entire phase of the outburst (see Fig. 2(a) and 2(b)).

To obtain a physical picture of the accretion flow dynamics of the source during its 2005 outburst, we refitted all spectra with the TCAF model based *fits* file as an additive table model in XSPEC. During spectral fit, we kept mass parameter frozen at $7\,M_\odot$ as this was the estimated mass value obtained from spectral analysis with the TCAF model during the 2000 outburst of the source (Paper-I). Throughout the observation period, the Keplerian disk rate ($\dot{m}_d$) was observed to be much less as compared to the sub-Keplerian halo rate ($\dot{m}_h$). This result is consistent with the non-requirement of the DBB component while fitting spectra with the PL model. On the first observation (MJD=53384.99) day, the value of $\dot{m}_d$ was $0.041\,\dot{M}_{\rm Edd}$. On the second observation day, it increased slightly ($\sim 0.044\,\dot{M}_{\rm Edd}$), and subsequently became roughly constant at that value except during the last few observations when a slow monotonic increase (up to $0.48\,\dot{M}_{\rm Edd}$) was observed. The sub-Keplerian halo rate ($\dot{m}_h$) manifested a monotonic decrease from 0.31 to $0.26\,\dot{M}_{\rm Edd}$ during the entire period of the outburst. The variations of $\dot{m}_d$ and $\dot{m}_h$ are plotted in Fig. 2(d)-(e). The variations of the TCAF model fitted shock parameters (location X_s and compression ratio R) are shown in Figure 2(f)-(g). On the first observation day, a strong shock ($R = 3.61$) at a far location ($X_s = 406\,r_s$) was observed. As the day progresses, the shock becomes weaker and moves inward. On the last observation day, a comparatively weaker shock ($R = 3.40$) at $X_s = 245\,r_s$ is observed.

Table 2 X-ray Flux Contributions of Total, Accretion disk and Jets

Obs Id. (1)	MJD (2)	F_X (3)	$F_{\rm inf}$ (4)	$F_{\rm ouf}$ (5)	% of $F_{\rm ouf}$ (6)	Norm (7)
X–01–00	53384.99	$0.767^{\pm 0.009}$	$0.308^{\pm 0.007}$	$0.459^{\pm 0.011}$	$59.84^{\pm 1.59}$	$10.93^{\pm 0.312}$
X–01–07	53385.65	$0.732^{\pm 0.009}$	$0.345^{\pm 0.007}$	$0.387^{\pm 0.011}$	$52.86^{\pm 1.63}$	$9.287^{\pm 0.299}$
X–01–02	53385.84	$0.700^{\pm 0.008}$	$0.306^{\pm 0.007}$	$0.394^{\pm 0.010}$	$56.28^{\pm 1.56}$	$9.981^{\pm 0.301}$
X–01–08	53386.35	$0.656^{\pm 0.009}$	$0.334^{\pm 0.007}$	$0.322^{\pm 0.011}$	$49.08^{\pm 1.80}$	$8.572^{\pm 0.309}$
X–01–09	53387.20	$0.598^{\pm 0.009}$	$0.302^{\pm 0.007}$	$0.296^{\pm 0.011}$	$49.49^{\pm 1.98}$	$8.650^{\pm 0.311}$
X–01–04	53387.80	$0.578^{\pm 0.008}$	$0.306^{\pm 0.005}$	$0.272^{\pm 0.009}$	$47.05^{\pm 1.68}$	$8.267^{\pm 0.312}$
X–01–05	53388.79	$0.535^{\pm 0.008}$	$0.308^{\pm 0.006}$	$0.227^{\pm 0.010}$	$42.42^{\pm 1.97}$	$7.581^{\pm 0.325}$
X–01–11	53389.13	$0.535^{\pm 0.007}$	$0.316^{\pm 0.004}$	$0.219^{\pm 0.008}$	$40.93^{\pm 1.58}$	$7.387^{\pm 0.297}$
X–01–12	53389.58	$0.519^{\pm 0.007}$	$0.315^{\pm 0.005}$	$0.204^{\pm 0.008}$	$39.30^{\pm 1.63}$	$7.209^{\pm 0.300}$
X–01–13	53390.09	$0.490^{\pm 0.006}$	$0.301^{\pm 0.006}$	$0.189^{\pm 0.008}$	$38.57^{\pm 1.69}$	$7.115^{\pm 0.297}$
X–01–06	53390.49	$0.478^{\pm 0.006}$	$0.295^{\pm 0.006}$	$0.183^{\pm 0.008}$	$38.28^{\pm 1.74}$	$7.075^{\pm 0.294}$
Y–02–00	53391.07	$0.419^{\pm 0.006}$	$0.263^{\pm 0.006}$	$0.156^{\pm 0.008}$	$37.23^{\pm 1.98}$	$6.992^{\pm 0.297}$
Y–02–02	53391.99	$0.377^{\pm 0.006}$	$0.246^{\pm 0.007}$	$0.131^{\pm 0.009}$	$34.74^{\pm 2.45}$	$6.686^{\pm 0.289}$
Y–02–03	53392.05	$0.386^{\pm 0.005}$	$0.243^{\pm 0.007}$	$0.143^{\pm 0.008}$	$37.04^{\pm 2.12}$	$6.940^{\pm 0.292}$
Y–02–04	53392.67	$0.326^{\pm 0.005}$	$0.223^{\pm 0.006}$	$0.103^{\pm 0.007}$	$31.59^{\pm 2.20}$	$6.392^{\pm 0.294}$
Y–02–06	53393.72	$0.273^{\pm 0.005}$	$0.218^{\pm 0.005}$	$0.055^{\pm 0.007}$	$20.14^{\pm 2.59}$	$5.472^{\pm 0.284}$
Y–02–14	53394.15	$0.251^{\pm 0.005}$	$0.196^{\pm 0.006}$	$0.055^{\pm 0.007}$	$21.91^{\pm 2.82}$	$5.608^{\pm 0.286}$
Y–02–15	53394.21	$0.244^{\pm 0.005}$	$0.190^{\pm 0.005}$	$0.054^{\pm 0.007}$	$22.13^{\pm 2.90}$	$5.593^{\pm 0.281}$
Y–02–07	53394.68	$0.218^{\pm 0.005}$	$0.186^{\pm 0.005}$	$0.032^{\pm 0.007}$	$23.39^{\pm 3.25}$	$5.133^{\pm 0.280}$
Y–02–09	53395.06	$0.198^{\pm 0.004}$	$0.177^{\pm 0.005}$	$0.021^{\pm 0.006}$	$10.60^{\pm 3.03}$	$4.498^{\pm 0.290}$
Y–02–10	53395.59	$0.185^{\pm 0.004}$	$0.183^{\pm 0.004}$	$0.002^{\pm 0.005}$	$1.081^{\pm 2.70}$	$4.413^{\pm 0.283}$

$X = 90011 - 01$ and $Y = 90111 - 01$ are prefixes of observation IDs. Total (F_X), accretion disk ($F_{\rm inf}$) and jet ($F_{\rm ouf}$) X-ray fluxes are in units of 10^{-9} erg cm^{-2} s^{-1} and they are calculated in the $3 - 25$ keV PCA band;
TCAF model fitted normalization (N) values with errors are listed in Col. (8);
The superscripts are average error values of the $\pm$ 90% confidence errors, extracted using the 'err' task in XSPEC.

3.3 Jet X-ray

Radio emission observed in BHCs is considered to be a tracer of jets and outflows. The strong radio emission is reported during most of the outburst (see Hynes et al. 2006; Maitra et al. 2009; Brocksopp et al. 2010). During the 2000 outburst, similar strong radio emission was observed (see *http://www.mrao.cam.ac.uk/~guy/J1118+480/J1118480.list*). It can be noted that the radio flux ($F_{\rm R}$) decreases as PCA rate decreases (see Fig. 3(e) and Fig. 2(a)). So, it appears that the outburst is totally dominated by the emission from jets/outflows. This motivated us to separate X-ray contribution from the jet/outflow ($F_{\rm ouf}$) from that of the accretion disk or inflowing matter ($F_{\rm inf}$) using the same method as described in JCD17 and Paper-I.

According to TCAF, model normalization parameter is a function of the mass of the BH ($M_{\rm BH}$), the inclination angle (i) and the distance (D) of the system. So when there is no prominent X-ray contribution from other physical processes (whose effects are not considered in the current version of the TCAF model fits file), for example, jets or outflows or precession in the disk, N should not vary from one day to another if observed with a given instrument. But during the outburst, we see a monotonic decrease in N from 10.9 to 4.41 (see Fig. 3(d)). Its variation is roughly similar to $F_{\rm R}$ (see Fig. 3(e)). This allows us to conclude that higher N values are possibly required to fit the spectra to match excess contribution of X-rays, emitted from the base of the jet.

Total X-ray fluxes (F_X) are obtained in our PCA spectral analysis band ($3 - 25$ keV), when all the TCAF model input parameters (except the mass of the BH) are kept free. In the presence of jet or outflow, F_X is the combined contribution of the radiations from the accretion disk and CENBOL, i.e. from inflowing matter ($F_{\rm inf}$) and from the base of the jet, i.e., from outflowing matter ($F_{\rm ouf}$). Significant X-ray contribution from the jet to the total X-ray influences our spectral fitting with the TCAF model. Since the present version of the TCAF model fits file only takes care of radiation contributed from the inflowing matter, higher values of normalization are required to fit the spectra to compensate the excess X-ray radiations emitted from the jet. In the absence of a jet, an almost constant value of model normalization is sufficient to fit the spectra during the entire outburst (see Molla et al. 2016, 2017; Chatterjee et al. 2016). For the case of the 2005 outburst of XTE J1118+480, we looked into the obtained N values and found that on the last date (MJD=53395.59), the model normalization was at its minimum value of 4.41. This implies that in this observation, total X-ray flux was contributed only by the radiations from the accretion disk and CENBOL. So, we may say that on this observation date X-ray emission from jets was minimum or negligible. This was indeed observed via variation of the radio fluxes (see Fig. 3(e)). So, after confirmation from low $F_{\rm R}$ at the

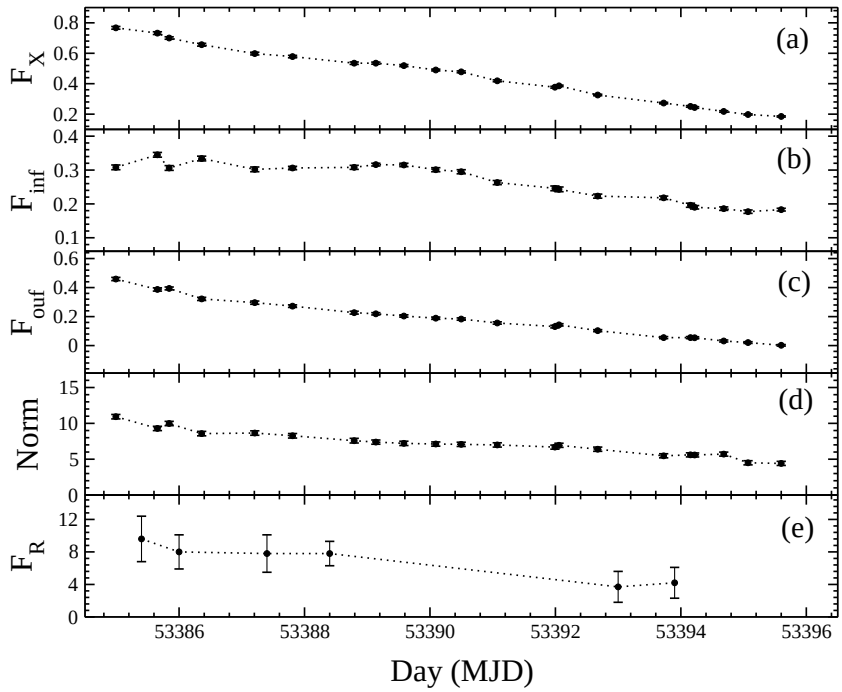

Fig. 3 Variation of (a) total flux (F_X), (b) inflow or disk flux ($F_{\rm inf}$), (c) outflow or jet flux ($F_{\rm ouf}$), (d) model normalization (N) and (e) radio flux ($F_{\rm R}$) are displayed with MJD. F_X, $F_{\rm inf}$ and $F_{\rm ouf}$ are obtained TCAF model fitted spectra in the $3-25$ keV PCA range in units of $10^{-9}\,{\rm erg\,cm^{-2}\,s^{-1}}$ unit. $F_{\rm R}$ of the 15 GHz Ryle Telescope is presented in the unit of mJy and adopted from Brocksopp et al. (2010).

lowest N observed day, we may obtain $F_{\rm inf}$ during the entire outburst by refitting spectra with the frozen model N value (at its lowest observed value, obtained when all model flow parameters are kept free). Now we can separate the jet component of the X-ray fluxes ($F_{\rm ouf}$) in each observation by subtracting $F_{\rm inf}$ from F_X (observed flux when all model flow parameters are kept free), i.e.,

$$F_{\rm ouf} = F_X - F_{\rm inf}\,. \qquad (1)$$

This method of separating jet contribution of X-ray from total observed X-ray was introduced in JCD17.

Although during the 2005 outburst of XTE J1118+480, the minimum N value 4.41 was required to fit spectra, according to Paper-I, the lowest N value that was required to fit the 2000 outburst spectra was 4.37. Since the Paper-I N value was lowest between two outbursts, to obtain X-ray contribution only from the disk and CENBOL, i.e., inflowing matter, we refitted all 2005 studied PCA spectra with the TCAF model after keeping model normalization frozen at 4.37. Finally, $F_{\rm ouf}$ is calculated for each observation by taking the difference of $F_{\rm inf}$ and F_X as in Equation (1). The evolutions of F_X, $F_{\rm inf}$, $F_{\rm ouf}$, N and $F_{\rm R}$ are depicted in Figure 3. $F_{\rm ouf}$ shows a similar variation as N and $F_{\rm R}$. When we see the percentage of jet X-ray contribution in total emitted X-ray, as an outburst progresses it decreases (see Col. (6) of Table 2). Maximum fractional jet X-ray contribution is found to be $\sim 60\%$.

4 SUMMARY AND DISCUSSIONS

The 2005 outburst of XTE J1118+480 (epoch under consideration here) is shorter duration, less intense and less studied compared to its earlier 2000 outburst. To understand the nature of the accretion flow dynamics of the source during this outburst, we use RXTE PCA and HEXTE combined data for our temporal and spectral analysis. We did not find any prominent signature of low frequency QPOs in the 0.01 s binned Fourier transformed PDS, although Shahbaz et al. (2005) reported a QPO at $\sim$ 2 mHz from the optical data in the quiescent state (June 2003), which is in between two outbursts of the source. The spectral analysis is done utilizing two types of models: the phenomenological PL model and physical TCAF solution based *fits* file. A total of 21 observed data of combined PCA and HEXTE spectra in the energy range of $3-100$ keV (except some observations where, due to low S/N, $3-40$ keV data are used) are chosen for spectral fittings from 2005 January 14 (MJD=53384.99) to January 25 (MJD=53395.59). Although triggering of the outburst was reported by Zurita et al. (2005b) on 2005 January 9, RXTE started monitoring it five days later. So, we missed an important rapidly evolving rising phase of the outburst.

The evolution of the average PCA rate in the $2-25\,$keV band implies that on the first observation day (MJD=53384.99), the source already passed its peak intensity (see, Fig. 2(a)). During the entire period of the outburst, the photon count was found to be monotonically decreasing. While fitting spectra with the PL model, we noticed the same behavior for the PL flux (see Fig. 2(b)). We tried to fit the spectra with combined DBB plus PL models, but 'ftest' suggests that the DBB component is insignificant. This means that during the entire outburst, non-thermal PL photons are highly dominant over the low or insignificant thermal disk component. PL model fitted photon index (Γ) values are obtained in a lower range ($\sim 1.75-1.87$), implying that during the entire phase of the outburst, the source was in the hard state. If we relook at the Γ values, we see an increasing trend in it (from 1.81 to 1.87), i.e., rise in softness in the late declining phase of the outburst. There is no physical explanation for this Γ from the PL model fitted spectral analysis.

During the entire outburst, high dominance of the sub-Keplerian halo rate ($\dot{m}_h$) over the Keplerian disk rate ($\dot{m}_d$) in the presence of a strong shock ($R > 3$) far away from the BH ($X_s > 245\,r_s$) is observed. But if we look into the evolution of accretion rates, in the late declining phase (specifically in the last observations) a slow rise in $\dot{m}_d$ is observed although $\dot{m}_h$ is decreased. This explains the gradual softening, i.e., increase in Γ in the late declining phase of the outburst. This feature is quite uncommon in an outburst of a transient BHC. This was due to the vanishing of the jet effect. A similar late softening was also observed due to the slow rise in $\dot{m}_d$ during the late declining phase of the 2000 outburst (Paper-I). So, the source has been consistently behaving in a non-conventional way even after a gap of five long years. This points to the fundamental configuration of the binary and compactness of the system.

Radio flares are believed to be a tracer of jets or outflows. Similar to the 2000 outburst, high radio fluxes are also observed during the current outburst of XTE J1118+480. $F_{\rm R}$ exhibited similar declining variation as that of PCA rate, PL flux and F_X. Now, when we looked at the TCAF model fitted N values, a similar nature of monotonically decreasing values (from 10.9 to 4.41) is observed. This means that higher N values were required to fit spectra when stronger jets were present. We estimated $F_{\rm inf}$ by refitting the spectra with N frozen at its minimum observed value ($= 4.37$) during its 2000 and 2005 outbursts (when spectral fits are done with all TCAF model parameters as free). We estimate the X-ray flux contribution from jets ($F_{\rm ouf}$) and find that the fractional jet X-ray contribution ($F_{\rm ouf}/F_X$) is maximum $\sim 60\%$. Evolution of $F_{\rm ouf}$ looks similar to $F_{\rm R}$. It can be noted that the outburst is suppressed with the decrease in $F_{\rm ouf}$. Therefore, similar to the 2000 outburst of XTE J118+480, this so-called 'failed outburst' could be termed a jet activity dominated outburst.

Acknowledgements This work made use of PCA and HEXTE data of NASA's RXTE satellite. Research of D. D. and S. K. C. is supported in part by the Higher Education Dept. of the Govt. of West Bengal, India. D. D. and S. K. C. also acknowledge partial support from ISRO sponsored RESPOND project (ISRO/RES/2/418/17-18) fund. D. C. and D. D. acknowledge support from DST/SERB sponsored Extra Mural Research project (EMR/2016/003918) fund. A. J. and D. D. acknowledge support from DST/GITA sponsored India-Taiwan collaborative project (GITA/DST/TWN/P-76/2017) fund. A. J. acknowledges CSIR SRF fellowship (09/904(0012)2K18 EMR-1) and post-doctoral fellowship of PRL, Ahmedabad, India. K. C. acknowledges support from DST/INSPIRE fellowship (IF 170233).

References

Aktar, R., Das, S., & Nandi, A. 2015, MNRAS, 453, 3414
Bhattacharjee, A., Banerjee, I., Banerjee, A., Debnath, D., & Chakrabarti, S. K. 2017, MNRAS, 466, 1372
Brocksopp, C., Jonker, P. G., Maitra, D., et al. 2010, MNRAS, 404, 908
Chakrabarti, S., & Titarchuk, L. G. 1995, ApJ, 455, 623 (CT95)
Chakrabarti, S. K. 1997, ApJ, 484, 313
Chakrabarti, S. K. 1999a, A&A, 351, 185
Chakrabarti, S. K. 1999b, Indian Journal of Physics Section B, 73B, 931
Chakrabarti, S. K., & Mandal, S. 2006, ApJL, 642, L49
Chatterjee, D., Debnath, D., Chakrabarti, S. K., Mondal, S., & Jana, A. 2016, ApJ, 827, 88
Chatterjee, D., Debnath, D., Jana, A., & Chakrabarti, S. K. 2019, Ap&SS, 364, 14 (Paper-I)
Chatterjee, K., Debnath, D., Chatterjee, D., et al. 2020, MNRAS, 493, 2452
Chattopadhyay, I., & Das, S. 2007, New Astron., 12, 454
Chaty, S., Haswell, C. A., Smith, G. P., Smail, I., & Hynes, R. I. 2000, IAU Circ., 7394, 3
Chaty, S., Haswell, C. A., Malzac, J., et al. 2003, MNRAS, 346, 689
Cook, L., Patterson, J., Buczynski, D., & Fried, R. 2000, IAU Circ., 7397, 2
Das, T. K., & Chakrabarti, S. K. 1999, Classical and Quantum Gravity, 16, 3879
Debnath, D., Chakrabarti, S. K., & Nandi, A. 2010, A&A, 520, A98
Debnath, D., Chakrabarti, S. K., & Nandi, A. 2013, Advances in Space Research, 52, 2143

Debnath, D., Chakrabarti, S. K., & Mondal, S. 2014, MNRAS, 440, L121
Debnath, D., Molla, A. A., Chakrabarti, S. K., & Mondal, S. 2015a, ApJ, 803, 59
Debnath, D., Mondal, S., & Chakrabarti, S. K. 2015b, MNRAS, 447, 1984
Debnath, D., Jana, A., Chakrabarti, S. K., Chatterjee, D., & Mondal, S. 2017, ApJ, 850, 92
Esin, A. A., McClintock, J. E., Drake, J. J., et al. 2001, ApJ, 555, 483
Garcia, M., Brown, W., Pahre, M., et al. 2000, IAU Circ., 7392, 2
Gelino, D. M., Balman, ş., Kızıloğlu, Ü., et al. 2006, ApJ, 642, 438
González Hernández, J. I., Rebolo, R., & Casares, J. 2012, ApJL, 744, L25
Haswell, C. A., Hynes, R. I., King, A. R., et al. 2000, IAU Circ., 7407, 1
Hynes, R. I., Mauche, C. W., Haswell, C. A., et al. 2000, ApJL, 539, L37
Hynes, R. I., Haswell, C. A., Cui, W., et al. 2003, MNRAS, 345, 292
Hynes, R. I., Robinson, E. L., Pearson, K. J., et al. 2006, ApJ, 651, 401
Jana, A., Debnath, D., Chakrabarti, S. K., Mondal, S., & Molla, A. A. 2016, ApJ, 819, 107
Jana, A., Chakrabarti, S. K., & Debnath, D. 2017, ApJ, 850, 91 (JCD17)
Jana, A., Debnath, D., Chakrabarti, S. K., et al. 2020a, arXiv:2006.03310
Jana, A., Debnath, D., Chakrabarti, S. K., & Chatterjee, D. 2020b, RAA (Research in Astronomy and Astrophysics), 20, 028
Khargharia, J., Froning, C. S., Robinson, E. L., & Gelino, D. M. 2013, AJ, 145, 21
Maitra, D., Markoff, S., Brocksopp, C., et al. 2009, MNRAS, 398, 1638
Markoff, S., Falcke, H., & Fender, R. 2001, A&A, 372, L25
Mauche, C., Hynes, R., Charles, P., & Haswell, C. 2000, IAU Circ., 7401, 2
McClintock, J., Garcia, M., Zhao, P., Caldwell, N., & Falco, E. 2000, IAU Circ., 7542, 1
McClintock, J. E., Garcia, M. R., Caldwell, N., et al. 2001a, ApJL, 551, L147
McClintock, J. E., Haswell, C. A., Garcia, M. R., et al. 2001b, ApJ, 555, 477
Molla, A. A., Debnath, D., Chakrabarti, S. K., Mondal, S., & Jana, A. 2016, MNRAS, 460, 3163
Molla, A. A., Chakrabarti, S. K., Debnath, D., & Mondal, S. 2017, ApJ, 834, 88
Mondal, S., Debnath, D., & Chakrabarti, S. K. 2014, ApJ, 786, 4
Mondal, S., Chakrabarti, S. K., & Debnath, D. 2016, Ap&SS, 361, 309
Patterson, J., Fried, R., Harvey, D., et al. 2000, IAU Circ., 7412, 2
Pooley, G. G., & Waldram, E. M. 2000, IAU Circ., 7390, 2
Pooley, G. G. 2005, The Astronomer's Telegram, 385, 1
Remillard, R., Garcia, M., Torres, M. A. P., et al. 2005, The Astronomer's Telegram, 384, 1
Remillard, R., Morgan, E., Smith, D., & Smith, E. 2000, IAU Circ., 7389, 2
Revnivtsev, M., Sunyaev, R., & Borozdin, K. 2000, A&A, 361, L37
Rupen, M. P., Dhawan, V., & Mioduszewski, A. J. 2005, The Astronomer's Telegram, 387, 1
Shahbaz, T., Dhillon, V. S., Marsh, T. R., et al. 2005, MNRAS, 362, 975
Shang, J.-R., Debnath, D., & Chatterjee, D., et al. 2019, ApJ, 875, 4
Taranova, O., & Shenavrin, V. 2000, IAU Circ., 7407, 2
Uemura, M., Kato, T., Matsumoto, K., et al. 2000, PASJ, 52, L15
Wagner, R. M., Foltz, C. B., Starrfield, S. G., & Hewett, P. 2000, IAU Circ., 7542, 2
Wagner, R. M., Foltz, C. B., Shahbaz, T., et al. 2001, ApJ, 556, 42
Wood, K. S., Ray, P. S., Bandyopadhyay, R. M., et al. 2000, ApJL, 544, L45
Wren, J., & McKay, T. 2000, IAU Circ., 7394, 4
Zurita, C., Muñoz-Darias, T., Martínez-Pais, I. G., et al. 2005a, The Astronomer's Telegram, 424, 1
Zurita, C., Rodríguez, D., Rodríguez-Gil, P., et al. 2005b, The Astronomer's Telegram, 383, 1
Zurita, C., Torres, M. A. P., Steeghs, D., et al. 2006, ApJ, 644, 432